ISSN 0023-1584, Kinetics and Catalysis, 2017, Vol. 58, No. 5, pp. 601–609. © Pleiades Publishing, Ltd., 2017.
Original Russian Text © M.A. Kerzhentsev, E.V. Matus, I.A. Rundau, V.V. Kuznetsov, I.Z. Ismagilov, V.A. Ushakov, S.A. Yashnik, Z.R. Ismagilov, 2017, published in Kinetika i Kataliz, 2017, Vol. 58, No. 5, pp. 614–622.

Development of a Ni–Pd/$CeZrO_2$/Al_2O_3 Catalyst for the Effective Conversion of Methane into Hydrogen-Containing Gas

M. A. Kerzhentsev[a], E. V. Matus[a, *], I. A. Rundau[a, b], V. V. Kuznetsov[a], I. Z. Ismagilov[a], V. A. Ushakov[a], S. A. Yashnik[a], and Z. R. Ismagilov[a, c]

[a] *Boreskov Institute of Catalysis, Siberian Branch, Russian Academy of Sciences, Novosibirsk, 630090 Russia*

[b] *Novosibirsk State Technical University, Novosibirsk, 630073 Russia*

[c] *Institute of Coal Chemistry and Chemical Materials Science, Siberian Branch, Russian Academy of Sciences, Kemerovo, 650000 Russia*

**e-mail: matus@catalysis.ru*

Received November 16, 2016

Abstract—The effects of the Pd content (0–1 wt %) and the synthesis method (joint impregnation with Ni + Pd and Pd/Ni or Ni/Pd sequential impregnation) on the physicochemical and catalytic properties of Ni–Pd/$CeZrO_2$/Al_2O_3 were studied in order to develop an efficient catalyst for the conversion of methane into hydrogen-containing gas. It was shown that variation in the palladium content and a change in the method used for the introduction of an active constituent into the support matrix make it possible to regulate the redox properties of nickel cations but do not affect the size of NiO particles (14.0 ± 0.5 nm) and the phase composition of the catalyst ($(\gamma + \delta)$-Al_2O_3, $CeZrO_2$ solid solution, and NiO). It was established that the activity of Ni–Pd catalysts in the reaction of autothermal methane reforming depends on the method of synthesis and increases in the following order: Ni + Pd < Ni/Pd < Pd/Ni. It was found that, as the Pd content of the Ni–Pd/$CeZrO_2$/Al_2O_3 catalyst was decreased from 1 to 0.05 wt %, the ability for self-activation, high activity, and operational stability of the catalyst under the conditions of autothermal methane reforming remained unaffected: at 850°C, the yield of hydrogen was ~70% at a methane conversion of ~100% during a 24-h reaction.

Keywords: Ni–Pd catalysts, aluminum oxide, autothermal reforming, methane, hydrogen

DOI: 10.1134/S002315841705010X

INTRODUCTION

Hydrogen is an important reagent for the chemical, petroleum, and food industries. The current global market of hydrogen is estimated at 55 million tons per annum, and its increase by 30% is expected in the near five years [1–3]. The general tendency toward deeper petroleum refining and the development of the production of ammonia, methanol, and synthetic liquid fuel are responsible for a steady increase in the consumption of hydrogen. Its active use within the framework of hydrogen-oriented power engineering along with traditional areas of application is predicted because hydrogen is considered as the most promising energy carrier due to its high fuel rating and ecological compatibility [4–6]. The main currently available technologies for the production of hydrogen on an industrial scale include the steam reforming of natural gas, the reforming of petrochemical waste gases, the gasification of coal, and the electrolysis of water [1]. The steam hydrocarbon reforming technology affords to 85% of the hydrogen produced and includes the following stages of synthesis gas generation (I) and water gas conversion (II) followed by the removal of impurities from hydrogen [7, 8]:

$$CH_4 + H_2O \leftrightarrow CO + 3H_2, \quad \Delta H^0_{298\,K} = +206\ \text{kJ/mol}, \qquad \text{(I)}$$

$$CO + H_2O \leftrightarrow CO_2 + H_2, \quad \Delta H^0_{298\,K} = -41\ \text{kJ/mol}. \qquad \text{(II)}$$

Because the steam reforming of methane is an endothermic reaction, heat supply from without is required. A more advantageous energy balance is reached in autothermal reforming (ATR), which additionally includes the following exothermic reactions of methane oxidation [9]:

$$CH_4 + 1/2O_2 \leftrightarrow CO + 2H_2, \quad \Delta H^0_{298\,K} = -44\ \text{kJ/mol}, \qquad \text{(III)}$$

$$CH_4 + 2O_2 \leftrightarrow CO_2 + 2H_2O, \quad \Delta H^0_{298\,K} = -802\ \text{kJ/mol}. \qquad \text{(IV)}$$

Bimetallic catalysts on different supports (Al_2O_3, La_2O_3, ZrO_2, $MgAl_2O_4$, and $Ce_{1-x}Zr_xO_2$) are effective catalytic systems for hydrocarbon reforming processes [10–22]. As a rule, nickel serves as the main constituent of an active component, and noble metals (0.1–2.0 wt % of Rh, Pd, Pt, Ir, and Ru) serve as promoting additives. As compared with the monometallic catalysts based on noble metals, bimetallic catalysts are characterized by smaller noble metal contents, which make their use more profitable. As a rule, a joint [18, 20, 23, 24] or sequential [25–27] impregnation method is used in the preparation of the Ni-containing bimetallic catalysts.

From an analysis of published data, it follows that the presence of a noble metal (1) stabilizes an active component in a reduced state to decrease the probability of catalyst deactivation due to the oxidation of the active component [15, 16], (2) decreases the rate of formation of carbonaceous deposits [17], and (3) increases the resistance of the catalyst to sulfur-containing compounds [18]. In addition to a change in the redox properties, the introduction of the second metal can exert an effect on the electronic structure [17] and dispersity [19] of the active component. Thus, for instance, Yoshida et al. [20] noted that the average particle size of Ni in the Ni–M/Al_2O_3 catalysts increased with the metal content for M = Pd, Rh, or Ru or, on the contrary, decreased in the case of M = Pt, Ir, and Au. In a comparative study of the Ni–M/Al_2O_3 bimetallic catalysts (M = Pd, Pt, Au, Ir, Rh, or Ru), Yoshida et al. [20] found that Pd is the most effective modifier, which increases the dispersity of Ni particles and the capability of Ni^{2+} to be reduced and suppresses the oxidation of Ni^0 in the course of the oxidative steam reforming of methane. Based on an EXAFS study, Yoshida et al. [20] concluded that an improvement in the characteristics of the catalyst upon the introduction of palladium was caused by the formation of Pd clusters, which interacted with the particles of Ni. In the case of a Ni–M/$CeZrO_2$ catalyst (M = Pt, Pd, Fe, and Ag), an additive of Ag was recommended as an optimum promoter [21]. According to Dantas et al. [21], the higher activity and operational stability of the Ni–Ag/$CeZrO_2$ sample in a CH_4 ATR reaction is related to its redox properties. It was found [22] that the activity of the Ni–M/La_2O_3 catalysts (M = Pt, Sn, Mo, Re, and Pd) in the CH_4 ATR reaction increases in the order Pt < Sn < Mo < Re < Pd, which correlates with an increase of the reducibility of Ni^{n+} cations in $LaNi_{1-x}M_xO_3$.

The degree of interaction between metals in the bimetallic catalysts is different depending on the chemical composition of the catalyst, its preparation method, and the conditions of its activation and operation [10, 11]. In the case of weak interaction between nickel and a promoting additive, monometallic particles were formed, whereas a surface or bulk alloy was formed in the case of strong interaction. It was established [28] that the structure of bimetallic particles in the 0.9Ni–0.1Pd/γ-Al_2O_3 catalyst depends on the preparation method: the enrichment of the surface of bimetallic particles in palladium, which ensured the stability of Ni–Pd particles to oxidation, was observed upon the sequential impregnation (in contrast to the joint impregnation). On the contrary, in the case of the 10.6Ni–0.2Pd/α-Al_2O_3 catalyst [24], the joint impregnation led to a higher surface concentration of palladium in the bimetallic particles and to improved process characteristics in the oxidative steam reforming of methane.

Thus, the type, concentration, and method of the introduction of a promoting additive vary over a wide range, and their optimum values depend on both the catalyst composition and the conditions of a catalytic reaction. This work is a continuation of studies on the development of an efficient catalyst for the conversion of methane into hydrogen-containing gas [22, 29–31], and it is dedicated to a systematic study of the physicochemical and catalytic properties of the Ni–Pd/$CeZrO_2$/Al_2O_3 catalysts for CH_4 ATR depending on the Pd content and method used for the introduction of an active component into the support matrix. The promoting additive and support composition were chosen based on the previously obtained data [22, 29–31] according to which Pd is the most effective additive (among Pt, Sn, Mo, Re, and Pd) [22] and Al_2O_3 modified with 10 wt % $Ce_{0.5}Zr_{0.5}O_2$ is an optimum support material among La_2O_3, $Ce_xGd_{1-x}O_y$, $Ce_xZr_{1-x}O_y$, $Ce_{0.5}Zr_{0.5}O_2/Al_2O_3$, and $La_2O_3/Ce_{0.5}Zr_{0.5}O_2/Al_2O_3$ [29–31]. In comparison with the previous works, we studied the Ni–Pd catalytic systems, which are characterized by low Pd content, and examined for the first time the effect of the composition of an active component and the method of synthesis on the capability of the Ni–Pd/$CeZrO_2$/Al_2O_3 catalysts to undergo self-activation.

EXPERIMENTAL

Catalyst Synthesis Procedure

The Ni–Pd/$CeZrO_2$/Al_2O_3 catalysts were obtained by the joint and sequential incipient wetness impregnation of the 10$CeZrO_2$/Al_2O_3 support, whose characteristics were reported preciously [29]. On the joint impregnation, the support was impregnated with an aqueous solution of a mixture of metal salts (nickel nitrate $Ni(NO_3)_2 \cdot 6H_2O$ and palladium nitrate $Pd(NO_3)_2$ with specified concentrations); the samples were dried under an IR lamp at 80–85°C and calcined in a muffle furnace at 500°C for 4 h. In the Pd/Ni sequential impregnation, the support was impregnated with an aqueous solution of nickel nitrate, dried, and then calcined at 500°C for 4 h. The resulting Ni/$CeZrO_2$/Al_2O_3 sample was impregnated with a solution of palladium nitrate. In the Ni/Pd

sequential impregnation, the order of supporting metal salts was changed: first, the support was impregnated with a solution of palladium nitrate; then, after intermediate heat treatment at 500°C for 4 h, the Pd/$CeZrO_2$/Al_2O_3 sample was impregnated with a solution of nickel nitrate. The final stage of the heat treatment of the catalysts obtained by the above method was the same as that for the catalysts synthesized by the joint impregnation method. In the designations of the samples, the numbers before Pd indicate its weight contents in the catalysts.

Physicochemical Methods of Catalyst Characterization

The concentrations of metals in the test catalysts were determined by X-ray spectral fluorescence analysis on an ARL ADVANT'X analyzer (ThermoTechno Scientific, Switzerland) with an Rh anode of the X-ray tube.

The textural characteristics of the catalysts (specific surface area (S_{BET}), pore volume (V_{pore}), and average pore diameter (D_{pore})) were studied on an ASAP 2400 automated volumetric instrument (Micromeritics, the United States) by the measurement and treatment of low-temperature nitrogen adsorption isotherms at 77 K.

The X-ray diffraction (XRD) analysis of the samples was carried out on an HZG-4C diffractometer (Freiberger Prazisionmechanik, Germany) in monochromatic CoK_α radiation (λ = 1.79021 Å). Phase composition was characterized based on the diffraction patterns obtained by scanning a region of the angles $2\theta = 10°–80°$ with a step of 0.1 deg and an accumulation time of 6–15 s. The sizes of coherent scattering regions (CSRs) in nickel oxide were calculated from the 2.0.0. diffraction peak broadening of a NiO phase; the CSR of Ni was found from the 2.0.0. peak of a nickel phase.

The high-resolution transmission electron microscopy (HR TEM) images were obtained on a JEM-2010 microscope (JEOL, Japan) with a lattice resolution of 0.14 nm at an accelerating voltage of 200 kV. The local elemental microanalysis of the samples was performed by energy-dispersive X-ray (EDX) spectrometry on an EDAX spectrometer (EDAX Inc., the United States) equipped with a Si(Li) detector with an energy resolution of no less than 130 eV. The samples for HR TEM were applied to perforated carbon substrates fixed on copper gauzes.

The temperature-programmed reduction with hydrogen (TPR-H_2) was accomplished in a flow reactor (inside diameter, 5 mm) in accordance with a previously published procedure [29].

The thermal analysis (differential thermal analysis (DTA), thermogravimetric analysis (TGA), and differential thermogravimetric analysis (DTG)) of the samples was carried out on a NETZSCH STA 449 C thermal analyzer (NETZSCH Geratebau GmbH, Germany) in a temperature range of 25–900°C with a heating rate of 10 K/min in an atmosphere of air.

Procedure for Studying the Activity of Catalysts

The activity of catalysts in an ATR reaction of CH_4 was studied in a quartz flow reactor (inside diameter, 14 mm) in accordance with a procedure described previously [30, 31] at atmospheric pressure, a temperature of 700–900°C, a gas flow rate of 200 mL_N/min, and the molar ratio between reagents $CH_4 : H_2O : O_2 : He = 1 : 1 : 0.75 : 2.5$. Before the beginning of an experiment, the catalyst was reduced in the flow of a 30% H_2/He mixture at 800°C and a gas flow rate of 100 mL_N/min for 2 h. The long-term tests of the samples in the CH_4 ATR reaction were conducted at a reaction temperature of 850°C without preliminary catalyst activation in hydrogen. The reaction mixture was analyzed with the aid of a QMS 300 mass-spectrometric analyzer (Stanford Research Systems, the United States).

RESULTS AND DISCUSSION

Physicochemical Properties of the Catalysts

According to the X-ray spectral fluorescence analysis data, the metal contents of all of the Ni–Pd/$CeZrO_2$/Al_2O_3 catalysts obtained were consistent with the calculated values: the Ni content was 10 ± 0.5 wt %, and the Pd contents were 0.05, 0.1, 0.2, 0.5, and 1.0 wt % depending on the sample.

From the results of investigating the samples by the low-temperature adsorption of nitrogen, it follows that the composition of catalysts and the method of their synthesis do not exert a considerable effect on the textural characteristics of the samples. The specific surface area of the catalysts calcined at 500°C was 75 ± 10 m^2/g, and the pore volume was ~0.3 cm^3/g.

An analysis of the diffraction patterns of Ni–Pd/$CeZrO_2$/Al_2O_3 showed that the formal cell parameter of aluminum oxide remained almost unchanged (a = 7.90 Å) upon the introduction of an active constituent into the support. The phases of $(\gamma + \delta)$-Al_2O_3, a solid solution based on CeO_2 (JSPDS 43-1002) and ZrO_2 (JSPDS 42-1164) related to the support, and the NiO phase (JSPDS 47-1049) of the active constituent were present in the composition of the samples. Furthermore, a highly dispersed PdO phase (JSPDS 43-1024) was observed in the samples with a Pd high content (1 wt %). The average particle size of nickel oxide in the Ni–Pd/$CeZrO_2$/Al_2O_3 test catalysts estimated according to the Scherrer equation showed that the CSR size of NiO was 14.0 ± 0.5 nm regardless of their composition and preparation method. The high dispersity of active constituent particles was also retained after the reduction of Ni–Pd/$CeZrO_2$/Al_2O_3 in 30% H_2/He at 800°C. In this case, the formation of a Ni

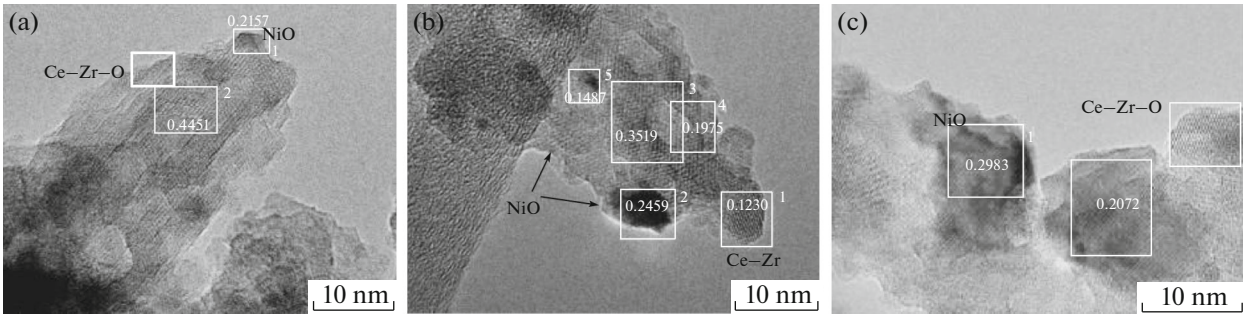

Fig. 1. HR TEM micrographs of the Ni–Pd/$CeZrO_2$/Al_2O_3 catalysts prepared by the Pd/Ni sequential impregnation method. Pd contents: (a) 0.05, (b) 0.2, and (c) 0.5 wt %.

metal phase (at a Pd content of <1 wt %) or a Ni–Pd alloy (at a Pd content of 1 wt %) with a particle size of 10.0 ± 1.0 nm. The evaluation of the presence of alloy at a low Pd content is difficult to perform because the determination of the cell parameter of Ni with a high accuracy is impossible due to the superposition of the lines of other phases.

According to the HR TEM data for the Ni–0.5Pd/$CeZrO_2$/Al_2O_3 catalysts obtained by both joint and sequential impregnation methods, the particles of $(Ce,Zr)O_2$ with a size of 2–10 nm were present on the surface of aluminum oxide [30]. The Ni-containing phase is formed by the particles of NiO and $NiAl_2O_4$ 10–15 nm in diameter. The Pd-containing phase predominantly occurs in a highly dispersed state and also in the form of PdO particles of size 2–3 nm. As can be seen in the micrographs of the Ni–Pd/$CeZrO_2$/Al_2O_3 samples (Fig. 1), the variation of the concentration of Pd does not lead to a change in the structure of the catalysts.

For studying the effects of the composition of the Ni–Pd/$CeZrO_2$/Al_2O_3 catalyst and its synthesis method on the reducibility of Ni^{n+} cations, the samples obtained were investigated by TPR-H_2. Figure 2a shows the TPR-H_2 curves for the Ni and Ni–Pd samples obtained by the Pd/Ni sequential impregnation method with different concentrations of palladium. The Ni/$CeZrO_2$/Al_2O_3 catalyst exhibited a wide peak with a maximum at 525°C due to the reduction of Ni^{2+} [11, 32, 33]. According to published data [33–35], the TPR-H_2 curves for the bulk NiO exhibited a peak of the absorption of hydrogen (T = 350 ± 20°C) or several peaks in the case of supported nickel oxide. Their positions depend on the composition of the support. It is well known [32] that the reduction of large NiO particles, which are characterized by weak metal–support interaction, occurs in a low-temperature region (T < 500°C), whereas the reduction of highly dispersed NiO particles, which are characterized by strong metal–support interaction, occurs in a high-temperature region (T > 500°C). Consequently, the strong metal–support interaction occurs in the Ni/$CeZrO_2$/Al_2O_3 catalyst, for which the reduction of nickel oxide is predominantly observed at T > 500°C.

The introduction of palladium changed the profile of the TPR-H_2 curve: a peak at T_1 ~ 50–150°C due to the reduction of palladium cations [1, 33] and a peak at T_2 ~ 400°C related to the reduction of nickel cations appeared. An increase in the palladium content led to an increase in the absorption of hydrogen in a temperature range of the second peak with a maximum at T_2 ~ 380–400°C and a decrease in the absorption of hydrogen in a high-temperature region with a maximum at T_3 ~ 550–570°C (Fig. 2a). The ratio of the peak areas with maximums at T_3 and T_2 decreased from 4.1 to 0.4 as the palladium content of the catalyst was increased from 0 to 0.5 wt %. This fact is indicative of a decrease in the fraction of difficult-to-reduce Ni^{2+} cations in the presence of Pd, apparently, due to the effect of spillover [11, 36]. The sample with a high content palladium (Ni–1.0Pd/$CeZrO_2$/Al_2O_3) in a temperature range of 300–800°C exhibited one peak of the absorption of hydrogen with a maximum at T_2 = 400°C.

Changes in the hydrogen absorption curve profile with increasing the Pd content of the sample were somewhat different upon varying the method of introducing metal precursors into the support matrix. In particular, two peaks of the absorption of hydrogen with maximums at T_2 ~ 400°C and T_3 ~ 550°C were detected in a region of 300–800°C for the catalysts obtained by the Pd/Ni sequential impregnation method at Pd concentrations of 0.2 wt % (Fig. 2b) and 0.5 wt % [30]. At the same time, in the samples prepared by the joint Pd + Ni and Ni/Pd sequential impregnation, one peak at T_2 ~ 400°C was detected, and the absorption of hydrogen in a high-temperature region increased insignificantly. As noted above, the curve of H_2 absorption by Ni–Pd/$CeZrO_2$/Al_2O_3 synthesized by the Pd/Ni sequential impregnation method exhibited only one peak at a Pd content of 1.0 wt %. Consequently, at a Pd concentration of <1.0 wt %, the fraction of difficult-to-reduce Ni^{2+} cations was higher in the samples obtained by the Pd/Ni sequential impregnation method than that in the samples synthe-

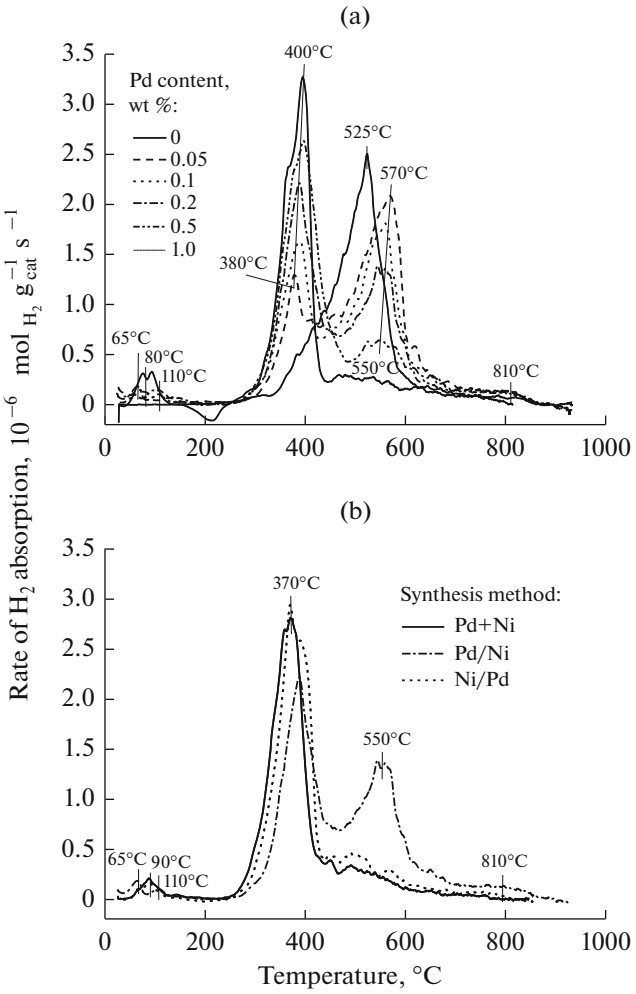

Fig. 2. TPR-H_2 curves of the Ni–Pd/$CeZrO_2$/Al_2O_3 samples: effects of (a) the Pd content of the Ni–Pd/$CeZrO_2$/Al_2O_3 catalyst obtained by the Pd/Ni sequential impregnation method and (b) the procedure of the preparation of the Ni–0.2Pd/$CeZrO_2$/Al_2O_3 catalyst on the absorption of hydrogen.

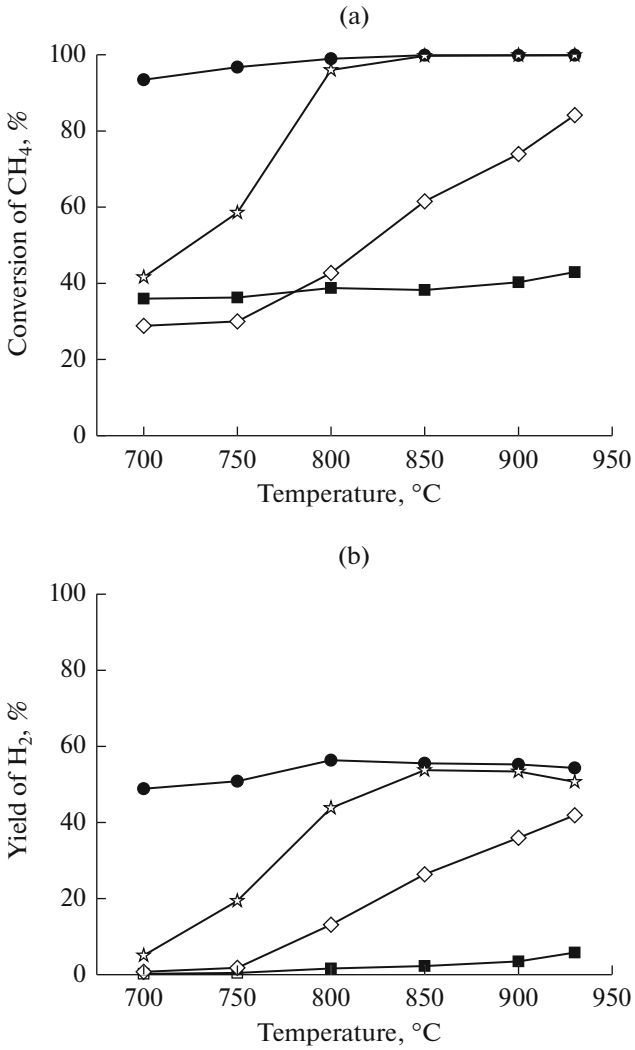

Fig. 3. The temperature dependence of (a) the conversion of methane and (b) the yield of hydrogen in the presence of the monometallic catalysts of the CH_4 ATR reaction. Sample compositions (■) $CeZrO_2/Al_2O_3$; (●) Ni/$CeZrO_2/Al_2O_3$; (◇) 0.05Pd/$CeZrO_2/Al_2O_3$; (☆) 1Pd/$CeZrO_2/Al_2O_3$.

sized by the joint or Ni/Pd sequential impregnation methods.

Thus, based on the study of the Ni–Pd/$CeZrO_2$/Al_2O_3 catalysts by a set of physicochemical methods (N_2 adsorption, XRD analysis, HR TEM, and TPR-H_2), we can conclude that the fraction of nickel cations, which are reduced in a low-temperature region (350–450°C), increases with the Pd content of the samples. In this case, the textural characteristics of the samples and their phase composition did not change. The exception was provided by the catalysts with high Pd content (1 wt %), in which the phases of highly dispersed PdO were formed. The variation of the method of introducing an active constituent into the support matrix also makes it possible to regulate the reducibility of the Ni^{2+} cations. The joint and Ni/Pd sequential impregnation methods (in comparison with the Pd/Ni sequential impregnation) ensured the almost complete absence of the difficult-to-reduce Ni^{2+} cations at a lower Pd content of the catalyst.

Activity of the Catalysts in the CH_4 ATR Reaction

Figure 3 illustrates the results of investigating the activity of monometallic catalysts in the CH_4 ATR reaction. In the case of the $CeZrO_2/Al_2O_3$ support, the conversion of CH_4 weakly depended on reaction temperature (700–950°C), and it was ~40%; the yield of H_2 was no higher than 5% (Fig. 3b), and the main reaction products were CO_2 and H_2O. The introduction of nickel led to a considerable increase in the conversion of CH_4 and the yield of H_2 (Fig. 3). These indices insignificantly increased with reaction temperature, and they were ~100 and 55%, respectively, at

Table 1. Activity of the Ni–Pd/$CeZrO_2$/Al_2O_3 catalysts in the CH_4 ATR reaction at 850°C

Pd content, wt %	Conversion of CH_4, %	Yield of H_2, %	Yield of CO, %	H_2/CO
Ni + Pd joint impregnation				
0.06	100	47	56	2.5
0.11	97	58	56	3.1
0.20	99	57	57	2.9
0.52	100	69	60	3.3
1.00	100	69	53	3.8
Pd/Ni sequential impregnation				
0.03	100	55	57	2.8
0.08	100	59	61	2.8
0.18	100	63	61	3.1
0.54	100	75	57	3.8
1.00	100	66	49	3.9
Ni/Pd sequential impregnation				
0.05	100	47	62	2.2
0.11	97	50	52	2.8
0.20	100	54	62	2.5
0.53	100	62	59	2.9
0.99	100	64	59	3.1

850°C. The main reaction products were H_2, CO, CO_2, and H_2O. In the presence of the Pd/$CeZrO_2$/Al_2O_3 catalysts, the temperature dependence of the conversion of CH_4 and the yield of H_2 was more pronounced: the process characteristics increased as the reaction temperature was increased (Fig. 3). As the palladium content of the Pd/$CeZrO_2$/Al_2O_3 catalyst was increased from 0.05 to 1.0 wt %, the catalyst activity increased. It should be noted that, as compared with Pd/$CeZrO_2$/Al_2O_3, the Ni/$CeZrO_2$/Al_2O_3 catalyst afforded better process characteristics for the ATR of CH_4. The activity of Ni/$CeZrO_2$/Al_2O_3 at 700–850°C was higher than or comparable with the activity of Pd/$CeZrO_2$/Al_2O_3 at 850–950°C.

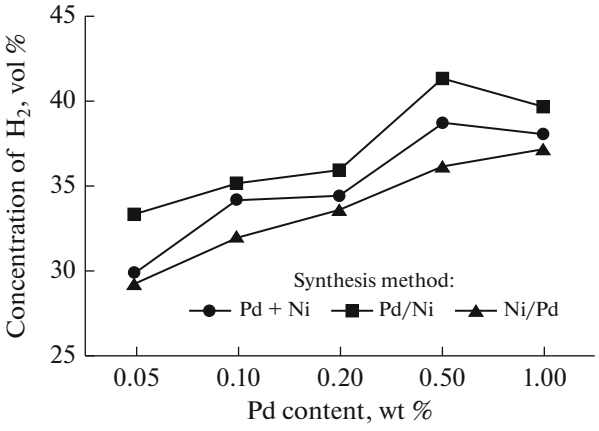

Fig. 4. Effect of the method of the synthesis of the Ni–Pd/$CeZrO_2$/Al_2O_3 catalysts on the concentration of hydrogen in the reaction mixture in the course of the CH_4 ATR reaction. T = 850°C.

For the bimetallic Ni–Pd catalysts, the temperature dependence of the CH_4 ATR process characteristics is analogous to that observed for the Ni catalyst: the conversion of CH_4 and the yield of H_2 insignificantly increased with the reaction temperature. In a wide temperature range (800–900°C), the Ni–Pd/$CeZrO_2$/Al_2O_3 catalysts ensured the yield of H_2 of no lower than 50% at a CH_4 conversion of >90%. An increase in the Pd content of the catalyst led to a certain increase in the yield of H_2 (see Table 1); with consideration for the TPR-H_2 data, this can be related to an improvement in the reducibility of nickel cations and, as a consequence, an increase in the number of Ni^0 active centers. This effect was maximally expressed in the samples obtained by the Pd/Ni sequential impregnation method. In particular, in the yield of H_2 at 850°C increased from 55 to 75% as the Pd content was increased from 0.05 to 0.5 wt % (see the table). The yield of H_2 also depended on the catalyst synthesis method. At the same chemical composition of the catalysts, the samples prepared by the Pd/Ni sequential impregnation method exhibited higher process characteristics (see Table 1 and Fig. 4).

We investigated the operational stability of the Ni–Pd/$CeZrO_2$/Al_2O_3 catalysts in the CH_4 ATR reaction depending on the composition and method used for

the introduction of an active constituent. Because the CH_4 ATR process characteristics in the presence of the Pd, Ni (Fig. 3), and Ni–Pd samples reached maximum values at a reaction temperature of 850°C and then remained unchanged with a further increase in the temperature, the long-term tests of the samples were conducted at $T = 850$°C. As noted above, in this case, the catalysts were tested without preliminary activation in hydrogen. From Fig. 5, it follows that the catalytic properties of the samples depend on the composition of an active constituent. In the case of the $Ni/CeZrO_2/Al_2O_3$ catalyst not modified with palladium, the conversion of CH_4 was only ~40%, and the yield of H_2 was lower than 3%. The products of the complete oxidation of methane—CO_2 and H_2O—were mainly formed. This fact is indicative of the absence of NiO reduction under the action of a reaction mixture under the CH_4 ATR reaction conditions. Indeed, according to the XRD analysis data, the Ni-containing phase in the $Ni/CeZrO_2/Al_2O_3$ sample after a 24-h reaction of the ATR of CH_4 was a solid solution phase with the structure of spinel ($NiO–Al_2O_3$, $a = 7.960$ Å). The preliminary treatment of the $Ni/CeZrO_2/Al_2O_3$ catalyst in hydrogen (30% H_2/He; 800°C; 2 h), which ensured the formation of a Ni^0 phase, led to its activation: the conversion of CH_4 increased to 100%, and the yield of hydrogen increased to 65%. However, the activity of this sample decreased in the course of time. In particular, the yield of H_2 was 65 or 50% after a 2- or 24-h reaction, respectively. Among the main reasons for the deactivation of Ni-containing catalysts in the processes of reforming are the oxidation and sintering of an active constituent, changes in the phase composition of the catalyst (for example, the formation of an inactive phase of nickel aluminate), and the formation of carbon deposits [11, 14].

In contrast to the $Ni/CeZrO_2/Al_2O_3$ sample, the $1.0Pd/CeZrO_2/Al_2O_3$ and $Ni–1.0Pd/CeZrO_2/Al_2O_3$ catalysts ensured the following stable process characteristics: the conversion of CH_4 was as high as 100%, and the yields of hydrogen were 55 and 70%, respectively (Figs. 5a, 5b). Note that preliminary treatment in hydrogen is not required for these samples. As can be seen in Fig. 5, at the initial stage of reaction (1–2 h), an increase in the process characteristics was observed. It is likely that the formation of a Ni metal or Ni–Pd alloy phase occurred during this period because of the reduction of Ni^{2+} cations under the action of a reaction mixture under the CH_4 ATR reaction conditions. As the Pd content of the $Ni–Pd/CeZrO_2/Al_2O_3$ catalyst was decreased from 1 to 0.05 wt %, both the catalyst capability for self-activation and the high yields of hydrogen (~70%) were retained (Fig. 5c). A study of the phase composition of the $Ni–Pd/CeZrO_2/Al_2O_3$ samples after a 24-h reaction showed that they contained a Ni–Pd alloy phase whose CSR size was 17 ± 3 nm regardless of the quantity of Pd. Accordingly, a decrease in the fraction of difficult-to-reduce Ni^{2+} cations upon the introduction of Pd into the composition of the catalysts, which was found using the TPR-

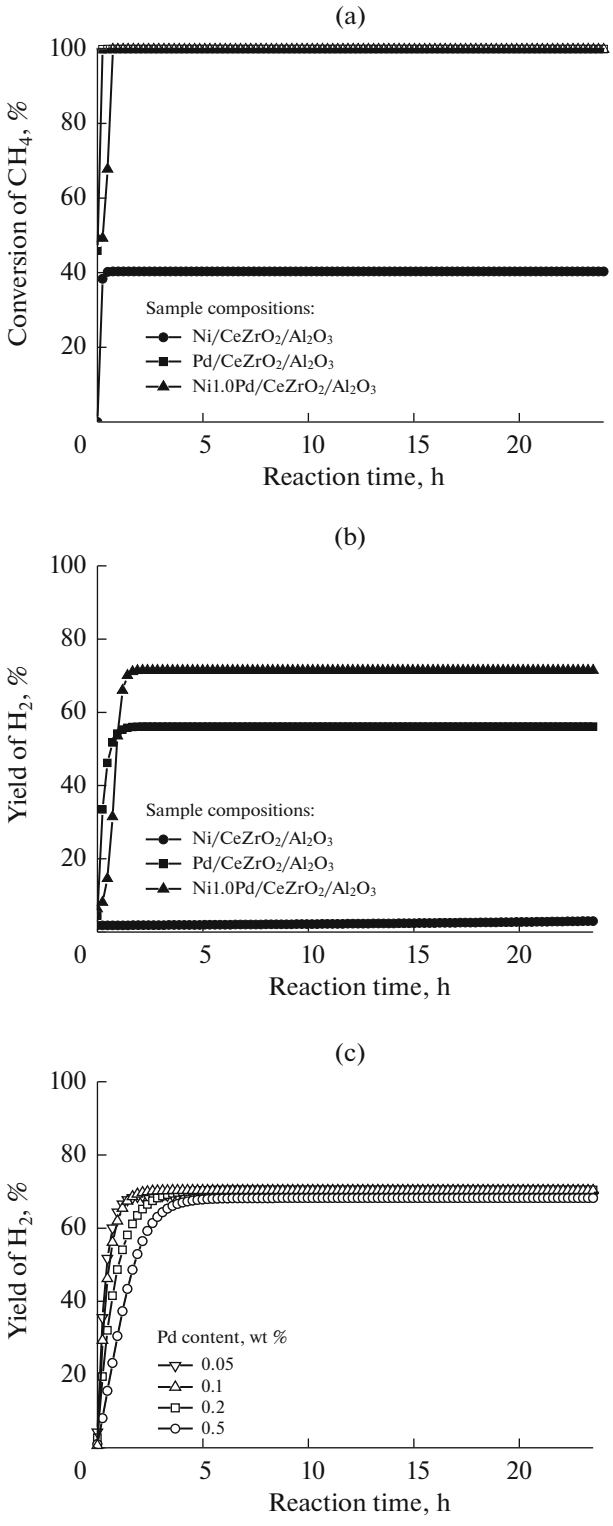

Fig. 5. Effect of the catalyst composition on the characteristics of the CH_4 ATR reaction. Preparation method: Pd/Ni sequential impregnation. $T = 850$°C.

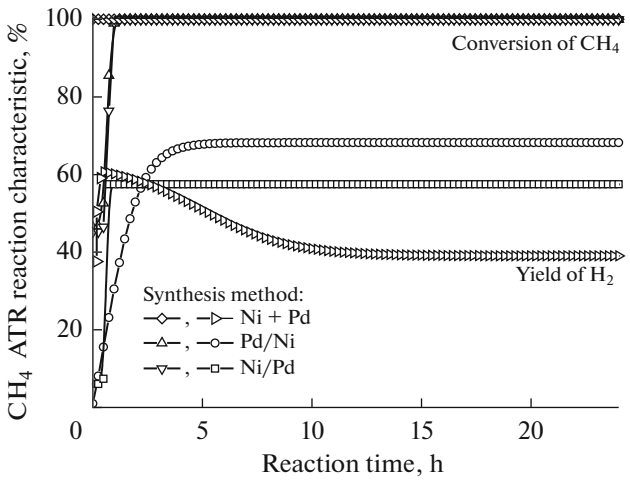

Fig. 6. Effect of the method of the preparation of the Ni–$0.5Pd/CeZrO_2/Al_2O_3$ catalysts on the characteristics of the CH_4 ATR reaction. $T = 850°C$.

H_2 method, facilitated the formation of active centers immediately under the conditions of the CH_4 ATR reaction; this makes it possible to exclude the stage of their preliminary treatment in a reducing atmosphere.

The activity of the Ni–$Pd/CeZrO_2/Al_2O_3$ catalysts depended on the method of introducing an of active constituent and increased in the following order: Ni + Pd < Ni/Pd < Pd/Ni (Fig. 6). The catalysts obtained by the sequential impregnation method stably operated under the CH_4 ATR reaction conditions. In their presence, the CH_4 ATR process characteristics—the conversion of CH_4, the concentration of H_2, and the yield of H_2—were close to equilibrium values: 100, 35–38, and 58–68%, respectively. In the case of the Ni–$Pd/CeZrO_2/Al_2O_3$ catalyst obtained by the joint impregnation method, the yield of hydrogen decreased from 60 to 40% for 24 h of reaction. Changes in the activity of the samples of Ni–$0.5Pd/CeZrO_2/Al_2O_3$ prepared by the joint impregnation method and $Ni/CeZrO_2/Al_2O_3$ with time were similar. Note that, according to the XRD data, the Ni–$0.5Pd/CeZrO_2/Al_2O_3$ catalysts synthesized by different methods were characterized by identical phase compositions after a 24-h reaction of the ATR of CH_4. According to published data [11], the joint impregnation method ensures the mixing of active constituent precursors on the molecular level already at the stage of support impregnation. This led to the formation of bimetallic particles with a uniform distribution of palladium and, as a result, caused a lowered surface concentration of Pd. In the sequential impregnation method, bimetallic particles with a high surface concentration of palladium (palladium clusters on the surface of Ni particles) were formed. At a higher surface concentration of Pd, the effect of promotion, namely, the stability of an active constituent to oxidation and the formation of carbon deposits, was more pronounced. In this connection, it is possible to assume that differences in the activity and operational stability of the Ni–$Pd/CeZrO_2/Al_2O_3$ catalysts obtained by different methods in the ATR of CH_4 were caused by the different structures of bimetallic particles.

The process characteristics reached (see the table and Fig. 5c) are comparable with or higher than those described in the literature [11, 21, 37–39]. This fact allowed us to consider the Ni–$0.05Pd/CeZrO_2/Al_2O_3$ catalyst as a promising catalytic system for the effective conversion of methane into hydrogen-containing gas.

CONCLUSIONS

Based on a systematic study of the physicochemical and catalytic properties of the Ni–$Pd/CeZrO_2/Al_2O_3$ catalysts depending on the Pd content (0–1 wt %) and the method of introducing an active constituent into the support matrix (Ni + Pd joint impregnation, Pd/Ni sequential impregnation, and Ni/Pd sequential impregnation), an optimum catalyst composition and a method of its preparation were determined. The Ni–$0.05Pd/CeZrO_2/Al_2O_3$ sample prepared by the Pd/Ni sequential impregnation method stably operated under CH_4 ATR reaction conditions and afforded a high yield of hydrogen (~70%) at a methane conversion of 100% and a reaction temperature of 850°C. Upon the introduction of Pd into the composition of the $Ni/CeZrO_2/Al_2O_3$ catalyst, the reducibility of Ni^{2+} cations was improved; this ensured the ability of Ni–Pd systems to be activated under the action of a reaction mixture in the CH_4 ATR reaction conditions.

ACKNOWLEDGMENTS

We are grateful to I.L. Kraevskaya, T.Ya. Efimenko, G.S. Litvak, and Cand. Sci. (Chem.) E.Yu. Gerasimov for their assistance in the characterization of the samples by physicochemical methods.

This work was performed within the framework of a state contract at the Boreskov Institute of Catalysis, Siberian Branch, Russian Academy of Sciences (project no. 0303-2016-0004).

REFERENCES

1. Navarro, R.M., Guil, R., and Fierro, J.L.G., in *Compendium of Hydrogen Energy,* vol. 1: *Hydrogen Production and Purification,* Amsterdam: Elsevier, 2015, p. 21.
2. Balat, M., *Int. J. Hydrogen Energy,* 2008, vol. 33, p. 4013.
3. Mueller-Langer, F., Tzimas, E., Kaltschmitt, M., and Peteves, S., *Int. J. Hydrogen Energy,* 2007, vol. 32, p. 3797.
4. Muradov, N.Z. and Veziroglu, T.N., *Int. J. Hydrogen Energy,* 2008, vol. 33, p. 6804.

5. Ball, M. and Wietschel, M., *Int. J. Hydrogen Energy,* 2009, vol. 34, p. 615.
6. Katikaneni, S.P., Al-Muhaish, F., Harale, A., and Pham, T.V., *Int. J. Hydrogen Energy,* 2014, vol. 39, p. 4331.
7. García, L., in *Compendium of Hydrogen Energy,* vol. 1: *Hydrogen Production and Purification,* Amsterdam: Elsevier, 2015, p. 83.
8. Holladay, J.D., Hu, J., King, D.L., and Wang, Y., *Catal. Today,* 2009, vol. 139, p. 244.
9. Arutyunov, V.S., *Okislitel'naya konversiya prirodnogo gaza* (Oxidative Reforming of Natural Gas), Moscow: Krasand, 2011.
10. Dal Santo, V., Gallo, A., Naldoni, A., Guidotti, M., and Psaro, R., *Catal. Today,* 2012, vol. 197, p. 190.
11. Nakagawa, D., Li, Y., and Tomishige, K., *Appl. Catal., A,* 2011, vol. 408, p. 1.
12. Angeli, S.D., Monteleone, G., Giaconia, A., and Lemonidou, A.A., *Int. J. Hydrogen Energy,* 2014, vol. 39, p. 1979.
13. LeValley, T.L., Richard, A.R., and Fan, M., *Int. J. Hydrogen Energy,* 2014, vol. 39, p. 16983.
14. Nahar, G. and Dupont, V., *Resent Pat. Chem. Eng.,* 2013, vol. 6, p. 8.
15. Li, D., Shishido, M., Oumi, Y., Sano, T., and Takehira, K., *Appl. Catal., A,* 2007, vol. 332, p. 98.
16. Miyata, T., Li, D., Shiraga, M., Shishido, T., Oumi, Y., Sano, T., and Takehira, K., *Appl. Catal., A,* 2006, vol. 310, p. 97.
17. Chin, Y.-H., King, D.L., Roh, H.-S., Wang, Y., and Heald, S.M., *J. Catal.,* 2006, vol. 244, p. 153.
18. Xie, C., Chen, Y., Li, Y., Wang, X., and Song, C., *Appl. Catal., A,* 2010, vol. 390, p. 210.
19. Luna, E.C., Becerra, A.M., and Dimitrijewits, M.I., *React. Kinet. Catal. Lett.,* 1999, vol. 67, p. 247.
20. Yoshida, K., Begum, N., Ito, S.-I., and Tomishige, K., *Appl. Catal., A,* 2009, vol. 358, p. 186.
21. Dantas, S.C., Escritori, J.C., Soares, R.R., and Hori, C.E., *Chem. Eng. J.,* 2010, vol. 156, p. 380.
22. Ismagilov, I.Z., Matus, E.V., Kuznetsov, V.V., Mota, N., Navarro, R.M., Yashnik, S.A., Prosvirin, I.P., Kerzhentsev, M.A., Ismagilov, Z.R., and Fierro, J.L.G., *Appl. Catal., A,* 2014, vol. 481, p. 104.
23. Garcia-Dieguez, M., Finocchio, E., Larrubia, M.A., Alemany, L.J., and Busca, G., *J. Catal.,* 2010, vol. 274, p. 11.
24. Yoshida, K., Okumura, K., Miyao, T., Naito, S., Ito, S.-I., Kunimori, K., and Tomishige, K., *Appl. Catal., A,* 2008, vol. 351, p. 217.
25. Lakhapatri, S.L. and Abraham, M.A., *Appl. Catal., A,* 2011, vol. 405, p. 149.
26. Morales-Cano, F., Lundegaard, L.F., Tiruvalam, R.R., Falsig, H., and Skjoth-Rasmussen, M.S., *Appl. Catal., A,* 2015, vol. 498, p. 117.
27. Gokaliler, F., Gocmen, B.A., and Aksoylu, A.E., *Int. J. Hydrogen Energy,* 2008, vol. 33, p. 4358.
28. Mukainakano, Y., Li, B., Kado, S., Miyazawa, T., Okumura, K., Miyao, T., Naito, S., Kunimori, K., and Tomishige, K., *Appl. Catal., A,* 2007, vol. 318, p. 252.
29. Ismagilov, I.Z., Matus, E.V., Nefedova, D.V., Kuznetsov, V.V., Yashnik, S.A., Kerzhentsev, M.A., and Ismagilov, Z.R., *Kinet. Catal.,* 2015, vol. 56, no. 3, p. 394.
30. Ismagilov, I.Z., Matus, E.V., Kuznetsov, V.V., Kerzhentsev, M.A., Yashnik, S.A., Prosvirin, I.P., Mota, N., Navarro, R.M., Fierro, J.L.G., and Ismagilov, Z.R., *Int. J. Hydrogen Energy,* 2014, vol. 39, p. 20992.
31. Ismagilov, I.Z., Matus, E.V., Kuznetsov, V.V., Mota, N., Navarro, R.M., Kerzhentsev, M.A., Ismagilov, Z.R., and Fierro, J.L.G., *Catal. Today,* 2013, vol. 210, p. 10.
32. Montoya, J.A., Romero-Pascual, E., Gimon, C., Del Angel, D., and Monzon, A., *Catal. Today,* 2000, vol. 63, p. 71.
33. Lisboa, J.S., Terra, L.E., Silva, P.R.J., Saitovitch, H., and Passos, F.B., *Fuel Process. Technol.,* 2011, vol. 92, p. 2075.
34. Abreu, A.J., Lucredio, A.F., and Assaf, E.M., *Fuel Process. Technol.,* 2012, vol. 102, p. 140.
35. Tsipouriari, V.A. and Verykios, X.E., *Catal. Today,* 2001, vol. 64, p. 83.
36. Dias, J.A.C. and Assaf, J.M., *Appl. Catal., A,* 2008, vol. 334, p. 243.
37. Wang, Y.H. and Zhang, J.C., *Fuel,* 2005, vol. 84, p. 1926.
38. Xiulan, C., Yuanxing, C., and Weiming, L., *J. Nat. Gas Chem.,* 2008, vol. 17, p. 201.
39. Hufschmidt, D., Bobadill, L.F., Romero-Sarria, F., Centeno, M.A., Odriozola, J.A., Montes, M., and Falabella, E., *Catal. Today,* 2010, vol. 149, p. 394.

Translated by V. Makhlyarchuk